ISA Transactions xxx (xxxx) xxx

Contents lists available at ScienceDirect

ISA Transactions

journal homepage: www.elsevier.com/locate/isatrans

Research article

Bilateral motion prediction and control for teleoperation under long time-varying delays

Shaobo Shen [a], Aiguo Song [a,*], Tao Li [b]

[a] School of Instrument Science and Engineering, Southeast University, Nanjing, 210096, China
[b] School of Automation Engineering, Nanjing University of Aeronautics and Astronautics, Nanjing, 211106, China

ARTICLE INFO

Article history:
Received 9 January 2020
Received in revised form 6 January 2021
Accepted 6 January 2021
Available online xxxx

Keywords:
Teleoperation
Time delay
Position tracking
Motion prediction

ABSTRACT

Bilateral controller design for the teleoperation system is studied in this paper based on a motion prediction approach. To compensate the known long time-varying delays, novel predictors are presented to reconstruct the positions and velocities of robots on both sides through using the delayed measurements. The proposed predictors consist of several sub-predictors in a cascade structure, each of which is to predict the states of the previous one. The estimations of the actual states can be obtained from the last sub-predictor. New prediction horizons of each sub-observers are designed to cope with the time-varying fractions of the time delay. Then through applying the predicted results, bilateral predictive controller is designed for the teleoperation. The errors of both position tracking and prediction can converge into the bounded regions under several sufficient conditions of the control gains, which are obtained by using the Lyapunov–Krasovskii approach. The effective capacity of the presented method can be verified through comparative simulations.

1. Introductions

With the developments of robotic and communication networks, teleoperation system has been widely developed to enable human operator to accomplish a work in distant. Since teleoperation systems are generally utilized in extensive fields, such as aerospace exploration, remote surgery, harmful chemical experiment, unmanned vehicles, and so on [1–3], they highly suffer from the time delays, which are hard to avoid owing to the long communication distance and bandwidth limitation [4]. Large communication delays can break down the real-time operation or even destabilize the robotic systems [5]. Recently, intensive research activities have been aiming to achieve the stable control for the bilateral teleoperations. Thus many important approaches have been proposed, such as wave variables [6], Lyapunov-based stability conditions [7], adaptive finite-time control method [8], and so on. It is worth mentioning that the delayed measurements have been directly used in most previous works of teleoperation system. The slave robot can just synchronize with the delayed positions of master robot, meanwhile the master side can only obtain a delayed feedback from the slave robot. However, in many practical applications of teleoperation system, the real-time motion synchronization and feedback are very essential [9]. Thus it is quite desirable to design a motion prediction method to reconstruct the real-time states of remote robot based on the delayed measurements.

In the case of linear teleoperation system, the motion prediction problems with constant time delay have been studied by utilizing the Smith predictor [10] and model predictive controller [11]. In [12], by considering delay as a constant with time-varying uncertainty, a time shift approach was proposed to estimate the system states of linear system with time-varying delayed output. For nonlinear robot systems, several motivated predictive controllers were proposed for robot systems with input time-delays [13,14]. However, the delayed measurements have not been considered. Recently, a number of observer-based approaches were presented to predict the actual states for unilateral robotic systems by using delayed measurements. For instance, in [15], the delayed output of the system were considered as special disturbances, which are estimated and compensated by applying extended state observers. In [16], a predictor with observer-based structure was proposed for a single robotic system with unilateral output delay. However, the bilateral motion prediction for nonlinear telerobotic system is still a challenging and open problem.

When the measurement (output) delay is enough small, we can just apply one predictor to predict the actual state of system [17]. Yet, in case of long time delay, we need to use several predictors with a cascade structure [18]. The cascade predictor is composed of a number of sub-predictors in a chain. Each sub-predictor is to predict the states of the previous one, and the

* Corresponding author.
E-mail addresses: shenshaobo@live.cn (S. Shen), a.g.song@seu.edu.cn (A. Song), autolitao@nuaa.edu.cn (T. Li).

https://doi.org/10.1016/j.isatra.2021.01.015
0019-0578/

last sub-predictor generates estimations of the actual states of the teleoperation system. In [17,19], the cascade predictors were applied to nonlinear system with invariable delays in output. In [20], output reconstruction methods were proposed, which turned the time-varying delayed output into constant delay cases through further delaying the measurements. But the prediction errors also rose due to the artificially increased delays. Then in [21], the cascade observer was designed to deal with a class of delayed measurements which were continuously available during some time horizons but sampled during others. Note that these approaches require the knowledge of controller inputs. However, as for teleoperation system, the predictors are located on the other sides of the robots to be estimated (as shown in Fig. 1). That is to say, the information of controller inputs cannot be immediately obtained and utilized by the predictors. Therefore, the cascade predictors in these approaches cannot be applied to handle the teleoperation systems directly. Besides, the controller design method based on the prediction results has not been considered in the mentioned previous works.

In this article, the design of bilateral predictor and controller for teleoperation systems under known communication delays are studied. A novel robust cascade prediction approach is proposed to estimate the real-time states of robots on both sides. Then motivated by [22], bilateral predictive controller is designed based on the existent prediction results. Through applying the Lyapunov–Krasovskii method, sufficient conditions guaranteeing the boundness of the prediction and tracking errors are obtained. Moreover, in uncertainty-free case, the prediction errors converge to zero exponentially. Finally, the performance of the designed controller and predictor is verified through comparative simulation results by using a two degree-of-freedom (DOF) teleoperation system.

The main novelties and contributions of this work are listed in the following:

1. Different from the previous cascade observers [17,19,20] with constant partitions of time delays and prediction horizons, we design new time-varying prediction horizons for the sub-observers to address the time-varying delays. Also we employ estimated input functions which can be obtained directly on the same side of the predictors, instead of the real inputs of the remote robot to be estimated. These features will greatly improve the convenience of implementation of the proposed predictors for teleoperation.
2. Based on the prediction results, bilateral predictive controller is designed for the teleoperation system. Differently from previous studies where the delayed measurements are directly used in the controllers [22–25], the proposed approach can ensure more timely information exchanging and more precise position synchronization between the robots.

2. Mathematical model and preliminaries

The n-DOF nonlinear teleoperation system which includes a master and a slave robot is described by

$$M_i(q_i)\ddot{q}_i + C_i(q_i, \dot{q}_i)\dot{q}_i = u_i + \varepsilon_i + f_i, \tag{1}$$

where $i = m, s$ indicates master or slave, $q_i, \dot{q}_i \in \Re^n$ are joint angles and velocities for the robots, respectively, u_i represents controller input, and ε_i represents the unknown disturbance. $f_m \in \Re^n$ represents the human operator input torque and $f_s \in \Re^n$ represents the environmental torque. $M_i(q_i) \in \Re^{n\times n}$ is the matrix of inertia, which is positive definite, and $C_i(q_i, \dot{q}_i) \in \Re^{n\times n}$ is the Coriolis and centrifugal effects matrix. Several common properties of the system are satisfied [23]:

P1: For some constants $\mu_{i1},\ \mu_{i2} > 0$, there is $\mu_{i2}I \geq M_i(q_i) \geq \mu_{i1}I$.

P2: For some constants $c_i > 0$, there is $\|C_i(q_i, \dot{q}_i)\| \leq c_i\|\dot{q}_i\|$.

P3: $\dot{M}_i(q_i) - 2C_i(q_i, \dot{q}_i)$ is skew symmetric.

As it is presented in Fig. 1, the robots on master and slave sides exchange messages to each other by communication channels under known time-varying forward delay $\tau_m(t)$ and feedback delay $\tau_s(t)$. We assume both positions and velocities are measurable. The first aim of our study is to design predictors to estimate the real-time states of robots on another side by utilizing the delayed outputs $q_i(t-\tau_i)$ and $\dot{q}_i(t-\tau_i)$. System (1) is initialized by $q_i(t) = 0$ and $\dot{q}_i(t) = 0$, whenever $t < 0$. Several assumptions on the time delays and unknown parts are given in the following.

Assumption 1. The unknown disturbances and inputs are bounded and satisfy

$$\|\varepsilon_i + f_i\| \leq v_1, \tag{2}$$

where $v_1 > 0$ is a constant, $\|\cdot\|$ represents the standard Euclidean norm,

Assumption 2. $\tau_m(t)$ and $\tau_s(t)$ are known, continuous, time-varying and bounded functions in time, which satisfy, for $i = m, s$,

$$\tau_0 \geq \tau_i(t) \geq \tau_1 \geq 0, \tag{3}$$

$$\dot{\tau}_i(t) < 1, \tag{4}$$

where τ_0, τ_1 are known upper and lower bounds of $\tau_i(t)$.

Remark 1. The assumptions on unknown parts and time delays are very commonly used in the designs of nonlinear systems [14, 23]. The assumption of known delay is realistic in many networked control applications. When clock synchronization can be achieved for robots at both sides, the time delays can be measured immediately by subtracting the time stamp of data packets [26]. Besides, for Internet-based communications, time delays change slower than the time thanks to communication protocols [27]. That is to say, the derivative of the delay is less than 1. Furthermore, once the time delays grow faster than the time, nothing new can be received from the communication channel. Under the circumstances, any remote control makes no sense. The upper and lower bounds of τ_m and τ_s could be different. For brevity, we can select τ_0 as the maximal upper bound, and τ_1 as the minimal lower bound of both τ_m and τ_s.

We reformulate the Eq. (1) as

$$\ddot{q}_i = M_i^{-1}(q_i)(u_i + \varepsilon_i + f_i) + g_i(q_i, \dot{q}_i), \tag{5}$$

where $g_i(q_i, \dot{q}_i) = -M_i^{-1}(q_i)C_i(q_i, \dot{q}_i)\dot{q}_i$. Because $M_i(\cdot)$ and $C_i(\cdot,\cdot)$ are usually very complex and hard to be determined or calculated for multi-degree of freedom robot, we will utilize the approximate functions in the prediction algorithm to render the proposed algorithm easily to be implemented.

Assumption 3. There exists available estimated functions $h_i(\cdot,\cdot)$ of $g_i(\cdot,\cdot)$ and $\hat{M}_i(\cdot)$ of $M(\cdot)$ which satisfy

$$\|h_i(q_i, \dot{q}_i) - g_i(q_i, \dot{q}_i)\| \leq v_2 \tag{6}$$

$$\bar{\mu}_{i1}I \leq \hat{M}_i(q_i) \leq \bar{\mu}_{i2}I. \tag{7}$$

where $v_2,\ \bar{\mu}_{i1}, \bar{\mu}_{i1} > 0$ are constants, and I represents the identity matrix.

Assumption 4. The first partial derivatives of $h_i(q_i, \dot{q}_i)$ and u_i are bounded.

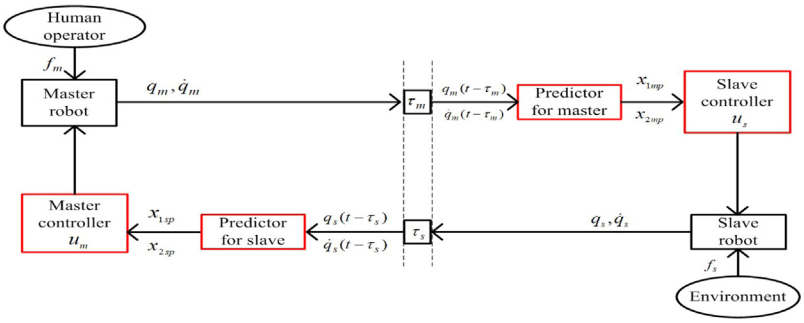

Fig. 1. The proposed control block for teleoperation.

Remark 2. The estimated functions in Assumption 3 are usually designed based on nominal parameters of the robot, such as in [25]. In our method, the predictors remain stable as long as $h_i(\cdot)$ and $M_i(\cdot)$ is bounded by conditions (6) and (7). The designs are relatively free. Nevertheless, better prediction results can be obtained by using more accurate estimated functions.

Let x_{1i} and x_{2i} denote the predicted position and velocity, respectively. In our method, we assume that the master controller is designed by using the measurements q_m, $\dot{q}_m$ and the predictions x_{1s}, x_{2s}, which can be obtained on the master side without delay. Similarly, the slave controller is designed by using q_s, $\dot{q}_s$ and the predictions x_{1m}, x_{2m}, That is

$$u_m = u_m(q_m,\ \dot{q}_m, x_{1s},\ x_{2s}) \tag{8}$$

$$u_s = u_m(q_s,\ \dot{q}_s, x_{1m},\ x_{2m}) \tag{9}$$

However, as is shown in Fig. 1, since the predictor is situated in the other side of the estimated robot, the controller u_i is unavailable in the predictor design. Thus, we will employ an estimated input function $\hat{u}_i$ based on the variables, which can be obtained directly on the same side of predictor. That is

$$\hat{u}_m = u_m(x_{1m},\ x_{2m}, q_s,\ \dot{q}_s) \tag{10}$$

$$\hat{u}_s = u_m(x_{1s},\ x_{2s}, q_m,\ \dot{q}_m) \tag{11}$$

3. Cascade predictors for teleoperation system

3.1. Partitions of time-varying delay and prediction horizons of sub-predictors

In the case of long time delay, we should use several sub-predictors in a cascade structure. Thus we divide the delay $\tau_i(t)$ into several partitions, and use the same numbers of sub-predictors to estimate the real positions gradually. Considering p_i numbers of partitions, where $p_i \geq 1$ is a positive integer for $i = m,\ s$, the following partition laws are applied to the presentation of proposed predictor [18]: for $j = 1, 2, \ldots, p_i$,

$$q_{ij}(t) = q_i\left(t - \tau_i(t) + j\frac{\tau_i(t)}{p_i}\right) \tag{12}$$

$$\dot{q}_{ij}(t) = \dot{q}_i\left(t - \tau_i(t) + j\frac{\tau_i(t)}{p_i}\right) \tag{13}$$

The structure of proposed cascade observer is given in Fig. 2, where the output of each sub-predictors x_{1ij}, x_{2ij} are estimations of q_{ij}, $\dot{q}_{ij}$, respectively. The actual states q_i and $\dot{q}_i$ will be estimated by the last predictor. Consequently, we have $x_{1i}(t) = x_{1i,j=p}(t)$ and $x_{2i}(t) = x_{2i,j=p}(t)$.

Each sub-predictor is to predict the positions of previous one with a prediction horizon $\zeta_{ij}(t)$. In other words, $x_{1ij}(t)$ is a prediction of $q_{ij}(t-\zeta_{ij}(t))$ which is approximatively replaced by $x_{1i,j-1}(t)$ in each sub-predictor. For a constant time delay $\tau_i(t) = \tau_{ic}$, we have $q_{ij}(t - \frac{1}{p_i}\tau_{ic}) = q_{i,j-1}(t)$. Thus we can use $\zeta_{ij}(t) = \frac{1}{p_i}\tau_{ic}$. But this relationship is incompatible for the time-varying delays. In our approach, motivated by [20], the update laws of time-varying delay horizons for sub-predictors are proposed as following:

$$\zeta_{ij}(t) = \left(1 - \frac{j-1}{p_i}\right)\tau_i(t) - T_{ij}(t), \tag{14}$$

$$T_{ij}(t) = \left(1 - \frac{j}{p_i}\right)\tau_i\left(t - \zeta_{ij}(t)\right). \tag{15}$$

Based on Eq. (12), the following relationship is checked:

$$\begin{aligned} q_{ij}(t-\zeta_{ij}(t)) &= q_i\left(t - \zeta_{ij}(t) - \left(1 - \frac{j}{p_i}\right)\tau_i(t-\zeta_{ij}(t))\right) \\ &= q_i\left(t - \left(1 - \frac{j-1}{p_i}\right)\tau_i(t) + T_{ij}(t) - T_{ij}(t)\right) \\ &= q_{i,j-1}(t) \end{aligned} \tag{16}$$

When the time delay is constant, from Eq. (14), we have $\zeta_{ij} = \frac{1}{p_i}\tau_{ic}$. In this case, the prediction horizons are same as the ones proposed for invariable delays [17–19].

Through differentiating both sides of (14), we can obtain

$$\begin{aligned} \dot{\zeta}_{ij}(t) &= \frac{\frac{p_i-j+1}{p_i}\dot{\tau}_i(t) - \frac{p_i-j}{p_i}\dot{\tau}_i\left(t-\zeta_{ij}(t)\right)}{1 - \frac{p_i-j}{p_i}\dot{\tau}_i\left(t-\zeta_{ij}(t)\right)}. \\ &= 1 - \frac{1 - \frac{p_i-j+1}{p_i}\dot{\tau}_i(t)}{1 - \frac{p_i-j}{p_i}\dot{\tau}_i\left(t-\zeta_{ij}(t)\right)}. \end{aligned} \tag{17}$$

Based on Assumption 2, since $\dot{\tau}_i(t) < 1$, there is

$$\dot{\zeta}_{ij}(t) < 1. \tag{18}$$

In addition, since $\tau_i(t)$ is bounded, ζ_{ij} is also bounded and satisfies, for all $j = 1, \ldots, p_i$,

$$0 \leq \zeta_{ij}(t) \leq \bar{\zeta}_i \tag{19}$$

where $\bar{\zeta}_i$ is the known upper bound of $\zeta_{ij}(t)$.

Remark 3. Based on Eqs. (14) and (15), $T_{ij}(t)$ and $\zeta_{ij}(t)$ can be built as shown in Fig. 3, which can be implemented using standard program "Variable Time Delay" in Matlab/Simulink.

3.2. Bilateral cascade predictor design

The proposed cascade predictor is presented as follows, for $j = 1, \ldots, p_i$,

$$\dot{x}_{1ij}(t) = l_{ij}(t)x_{2ij}(t), \tag{20}$$

$$\begin{aligned} \dot{x}_{2ij}(t) =& l_{ij}(t)[h_i(x_{1ij}(t), x_{2ij}(t)) + \hat{M}_i^{-1}(x_{1ij}(t))\hat{u}_{ij}(t)] \\ &+ K_{pi}(1 - \dot{\zeta}_{ij}(t))r_{ij\zeta}(t), \end{aligned} \tag{21}$$

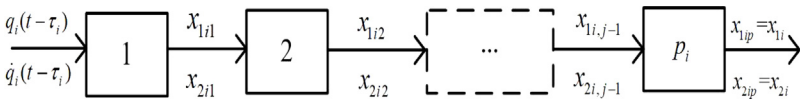

Fig. 2. The structure of cascade predictor.

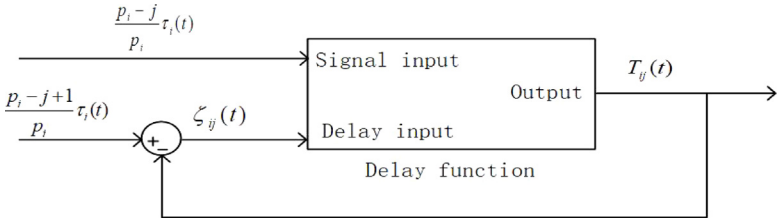

Fig. 3. The implementation of update law of prediction horizons.

where $x_{1ij}(t)$ and $x_{2ij}(t)$ are predictions of $q_{ij}(t)$ and $\dot{q}_{ij}(t)$ respectively, $l_{ij}(t) = [1-(1-j/m)\dot{\tau}_i(t)]$, K_{pi} is the positive constant predictor gain which can be expanded as

$$K_{pi} = k_a + k_b + k_c + k_{di}, \text{ for } i = m,\ s. \tag{22}$$

and for $j = 1$,

$$\begin{aligned} r_{i1\zeta}(t) =& \dot{q}_i(t-\tau_i) - x_{2ij}(t-\zeta_{i1}) + \alpha(q_i(t-\tau_i) - x_{1ij}(t-\zeta_{i1})) \\ & - K_{pi}\int_{t-\zeta_{ij}(t)}^{t}(1-\dot{\zeta}_{ij}(t))r_{ij\zeta}(\sigma)d\sigma, \end{aligned} \tag{23}$$

for $j = 2, \ldots, p_i$,

$$\begin{aligned} r_{ij\zeta}(t) =& x_{2i,j-1}(t) - x_{2ij}(t-\zeta_{ij}(t)) + \alpha(x_{1i,j-1}(t) - x_{1ij}(t-\zeta_{ij}(t))) \\ & - K_{pi}\int_{t-\zeta_{ij}(t)}^{t}(1-\dot{\zeta}_{ij}(t))r_{ij\zeta}(\sigma)d\sigma, \end{aligned} \tag{24}$$

We introduce the notations of prediction errors as following:

$$r_{ij\zeta}(t) = r_{ij}(t-\zeta_{ij}(t)), \tag{25}$$

$$e_{ij}(t) = q_{ij}(t) - x_{1ij}(t), \tag{26}$$

$$\eta_{ij}(t) = \dot{q}_{ij}(t) - x_{2ij}(t), \tag{27}$$

$$\theta_{ij}(t) = K_{pi}\int_{t-\zeta_{ij}(t)}^{t} r_{ij}(\sigma)d\sigma \tag{28}$$

$$R_{ij} = \eta_{ij}(t) + \alpha e_{ij}(t) - \theta_{ij}(t). \tag{29}$$

Notice that $\theta_{ij}(t-\zeta_{ij}(t)) = K_{pi}\int_{t-\zeta_{ij}(t)}^{t}(1-\dot{\zeta}_{ij}(t))r_{ij\zeta}(\sigma)d\sigma$. For $j = 1$, since $q_{i1}(t-\zeta_{i1}(t)) = q_i(t-\tau_i)$, we can conclude that

$$R_{i1}(t) = r_{i1}(t). \tag{30}$$

And for $j = 2, 3, \ldots, p_i$, since $q_{ij}(t-\zeta_{ij}(t)) = q_{i,j-1}(t)$, there is

$$R_{ij}(t-\zeta_{ij}(t)) = r_{ij}(t-\zeta_{ij}(t)) + \eta_{i,j-1}(t) + \alpha e_{i,j-1}(t). \tag{31}$$

After defining $\Omega_{ij}(t) = t - \zeta_{ij}(t)$, there is

$$R_{ij}(t) = r_{ij}(t) + E_{ij}(t). \tag{32}$$

where

$$E_{ij}(t) = \eta_{i,j-1}(\Omega_{ij}^{-1}(t)) + \alpha e_{i,j-1}(\Omega_{ij}^{-1}(t)). \tag{33}$$

Theorem 1. *For cascade predictor (20)–(21) and the teleoperation system (1), if the gain K_{pi} are selected sufficiently large, such that for $j = 1, 2, \ldots, p_i$,*

$$k_a > \frac{\delta}{2},\ k_b > \frac{\rho_j^2(\|z_j(0)\|)}{2\phi_j},\ k_{di} > \frac{\delta + 2\omega + 2\kappa\bar{\zeta}_i}{2(1-\delta)}, \tag{34}$$

and if the prediction horizon are sufficient small such that following relations are simultaneously satisfied

$$\alpha > \frac{\delta}{2}, \tag{35}$$

$$\frac{\delta}{2\omega} < 1 - \dot{\zeta}, \tag{36}$$

$$\bar{\zeta}_i < \frac{2\kappa\delta}{3K_{pi}^2}, \tag{37}$$

then the prediction errors R_{ij}, e_{ij}, and η_{ij} converge to the bounded regions, where δ, ω, κ, γ_1, ϕ_j and γ_2 are a positive constants which will be specified later, $\rho(\cdot)$ represent a non-decreasing and positive function, $z_j(0)$ is the initial value of $z_j(t)$, and $z_j(t) \in \Re^{6n}$ is defined as

$$z_j(t) = \begin{bmatrix} e_{mj}^T & \theta_{mj}^T & R_{mj}^T & e_{sj}^T & \theta_{sj}^T & R_{sj}^T \end{bmatrix}^T. \tag{38}$$

Proof of Theorem 1. Throughout this proof, the time argument t is omitted for brevity.

By substituting Eqs. (26)–(28) into (29), the time derivative of R_{ij} can be obtained as

$$\begin{aligned} \dot{R}_{ij} =& l_{ij}\ddot{q}_{ij} - \dot{x}_{2ij} + \alpha\dot{e}_{ij} + K_{pi}(1-\dot{\zeta}_{ij})r_{ij\zeta} - K_{pi}r_{ij} \\ =& l_{ij}\ddot{q}_{ij} + \alpha\dot{e}_{ij} - l_{ij}[h(x_{1ij}, x_{2ij}) - \hat{M}_i^{-1}(x_{1ij})\hat{u}_{ij}] - K_{pi}r_{ij}. \end{aligned} \tag{39}$$

According to Eq. (5) and relationships (30) and (32), we have

$$\dot{R}_{ij} = \begin{cases} N_{dij} + N_{ij} - e_{ij} - K_{pi}R_{ij}, & \text{for } j = 1, \\ N_{dij} + N_{ij} - e_{ij} - K_{pi}(R_{ij} + E_{ij}), & \text{for } j = 2, \ldots, p_i, \end{cases} \tag{40}$$

where

$$N_{dij} = l_{ij}[M_i^{-1}(q_{ij})(\varepsilon_i + f_i) + g_i(q_{ij}, \dot{q}_{ij}) - h_i(q_{ij}, \dot{q}_{ij})] \tag{41}$$

$$\begin{aligned} N_{ij} =& l_{ij}[h_i(q_{ij}, \dot{q}_{ij}) - h_i(x_{1ij}, x_{2ij}) + \\ & M_i^{-1}(q_{ij})u_{ij} - \hat{M}_i^{-1}(x_{1ij})\hat{u}_{ij} + \alpha\eta_{ij}] + e_{ij}. \end{aligned} \tag{42}$$

Based on Property 1, Assumptions 1 and 3, N_{dij} can be upper bounded as

$$\|N_{dij}\| \le \upsilon = \upsilon_1/\mu_1 + \upsilon_2, \tag{43}$$

And the upper bound of N_{ij} can be derived according to the Mean Value Theorem as [13]:

$$\|N_{ij}\| \le \rho_j(\|z_j\|)\|z_j\|, \tag{44}$$

In view of the definition of u_m in (8) and $\hat{u}_m$ in (10), the boundness of $M_m^{-1}(q_{mj})u_{mj} - \hat{M}_m^{-1}(x_{mj})\hat{u}_{mj}$ is determined by not only e_{mj}^T and R_{mj}^T, but also e_{sj}^T and R_{sj}^T. And it is the same as for u_s and $\hat{u}_s$. Thus for both N_{mj} and N_{sj}, their bounds should be determined by the functions of $\|z_j\|$ which contains the prediction

errors of predictors on both sides. Hence, the stability for the master and slave predictors cannot be separately analyzed.

For $j = 1, 2, \ldots, p_i$, the following Lyapunov–Krasovskii functional is established:

$$W_j = V_{mj} + V_{sj}, . \tag{45}$$

$$V_{ij} = \frac{1}{2}e_{ij}^T e_{ij} + \frac{1}{2}R_{ij}^T R_{ij} + \frac{1}{2K_{pi}}\theta_{ij}^T\theta_{ij} + Q_{ij} + P_{ij}, \text{ for } i = m,\ s. \tag{46}$$

where

$$Q_{ij} = \kappa\int_{t-\bar{\zeta}_i}^{t}\int_{s}^{t}\|r_{ij}(\sigma)\|^2 d\sigma ds \le \kappa\bar{\zeta}_i\int_{t-\bar{\zeta}_i}^{t}\|r_{ij}(\sigma)\|^2 d\sigma, \tag{47}$$

$$P_{ij} = \omega\int_{t-\zeta_{ij}}^{t}\|r_{ij}(\sigma)\|^2 d\sigma. \tag{48}$$

Let $y_j \in \Re^{10n}$ be defined as

$$y_j = \begin{bmatrix} e_{mj}^T & R_{mj}^T & \theta_{mj}^T & \sqrt{P_{mj}} & \sqrt{Q_{mj}} & e_{sj}^T & R_{sj}^T & \theta_{sj}^T & \sqrt{P_{sj}} & \sqrt{Q_{sj}} \end{bmatrix}^T, \tag{49}$$

then W_j can be bounded as

$$\lambda_1\|y_j\|^2 \le W_j(y,t) \le \lambda_2\|y_j\|^2. \tag{50}$$

where $\lambda_1 = min\left\{\frac{1}{2},\ \frac{1}{2K_{pi}}\right\}$, and $\lambda_2 = max\left\{1,\ \frac{1}{2K_{pi}}\right\}$

Through taking the time derivative of V_{ij}, there is

$$\begin{aligned}\dot{V}_{ij} =& l_{ij}e_{ij}^T(R_{ij} - \alpha e_{ij} - \theta_{ij}) + R_{ij}^T(N_{ij} + N_{dij} - e_{ij} - K_{pi}r_{ij}) \\ &+ \theta_{ij}^T(r_{ij\zeta} - r_{ij}) + \kappa\bar{\zeta}_i\|r_{ij}\|^2 - \kappa\int_{t-\bar{\zeta}_i}^{t}\|r_{ij}(\sigma)\|^2 d\sigma \\ &+ \omega(\|r_{ij}\|^2 - (1-\dot{\zeta})\|r_{ij\zeta}\|^2).\end{aligned} \tag{51}$$

The proof of the convergence of the cascade predictor will be presented in two steps. Firstly, the convergence of $e_{i1},\ s_{i1}$ will be shown. Then we shall prove the boundness of $e_{ij},\ s_{i1}$ provided that $e_{i,j-1},\ s_{i,j-1}$ is bounded.

Step 1: Using Young's inequality [7], we can check that

$$\|l_{ij}e_{ij}^T\theta_{ij}\| \le \frac{\delta}{2}l_{ij}^2\|e_{ij}\|^2 + \frac{1}{2\delta}\|\theta_{ij}\|^2, \tag{52}$$

$$\|\theta_{ij}^T r_{ij\zeta}\| \le \frac{\delta}{2}\|r_{ij\zeta}\|^2 + \frac{1}{2\delta}\|\theta_{ij}\|^2 \tag{53}$$

$$\|\theta_{ij}^T r_{ij}\| \le \frac{\delta}{2}\|r_{ij}\|^2 + \frac{1}{2\delta}\|\theta_{ij}\|^2 \tag{54}$$

Then we use the Cauchy–Schwarz inequality to derive

$$\|\theta_{ij}\|^2 \le \zeta_{ij}K_{pi}^2\int_{t-\zeta_{ij}}^{t}\|r_{ij}(\sigma)\|^2 d\sigma \le \bar{\zeta}_i K_{pi}^2\int_{t-\bar{\zeta}_i}^{t}\|r_{ij}(\sigma)\|^2 d\sigma, \tag{55}$$

For $j = 1$, since $r_{i1} = R_{i1}$, after applying (52)–(55) and (43)–(44) to (51), we have

$$\begin{aligned}\dot{V}_{i1} \le& -l_{ij}(\alpha - \frac{\delta}{2}l_{ij})\|e_{ij}\|^2 + \|R_{i1}\|\rho_1(\|z_1\|)\|z_1\| \\ &-(k_a + k_b + k_c)\|R_{i1}\|^2 \\ &+ \|R_{i1}\|v - (k_{di} - \frac{\delta}{2} - \omega - \kappa\bar{\zeta}_i)\|r_{i1}\|^2 \\ &-(\omega - \omega\dot{\zeta}_{ij} - \frac{\delta}{2})\|r_{i1\zeta}\|^2 \\ &-\left(\frac{\kappa}{\bar{\zeta}_i K_{pi}^2} - \frac{3}{2\delta} - \gamma_1^2 - \gamma_2^2\right)\|\theta_{i1}\|^2 \\ &-\bar{\zeta}_i(\gamma_1^2 + \gamma_1^2)\int_{t-\bar{\zeta}_i}^{t}\|r_{i1}(\sigma)\|^2 d\sigma.\end{aligned} \tag{56}$$

Then by substituting (56) into (45) and completing the squares, we have

$$\begin{aligned}\dot{W}_1 =& \dot{V}_{m1} + \dot{V}_{s1} \\ \le& -\left[\phi_1 - \frac{\rho_1^2(\|z_1\|)}{2k_b}\right]\|z_1\|^2 \\ &-\frac{\gamma_1^2}{\kappa}(Q_{m1} + Q_{s1}) - \frac{\bar{\zeta}_m\gamma_2^2}{\omega}P_{m1} - \frac{\bar{\zeta}_s\gamma_2^2}{\omega}P_{s1} + \frac{v^2}{2k_c}, \\ \le& -\frac{\bar{\phi}_1}{\lambda_2}W_1 + \frac{v^2}{2k_c}\end{aligned} \tag{57}$$

where

$$\phi_1 = \min_{i=m,\ s}\left\{l_{i1}(\alpha - \frac{\delta}{2}l_{i1}),\ k_a,\ \frac{\kappa}{\bar{\zeta}_i K_{pj}^2} - \frac{3}{2\delta} - \gamma_1^2 - \gamma_2^2\right\}, \tag{58}$$

$$\bar{\phi}_1 = \min_{i=m,\ s}\left\{\phi_1 - \frac{\rho_1^2(\|z_1\|)}{2k_b},\ \frac{\gamma_1^2}{\kappa},\ \frac{\bar{\zeta}_i\gamma_2^2}{\omega}\right\}. \tag{59}$$

Using the comparison lemma [28], we can get

$$W_1 \le W(0)e^{-\frac{\bar{\phi}_1}{\lambda_2}t} + \frac{v^2\lambda_2}{2k_c\bar{\phi}_1} \tag{60}$$

Based on definition of W_1, it can be concluded that R_{i1}, e_{i1}, and θ_{ij} converge into the bounded regions, provided that conditions (34)–(37) are satisfied.

Step j: In the next step, for $j = 2, \ldots, p_i$, based on the relationship (32), we have

$$\begin{aligned}-k_{di}\|R_{ij}\|^2 =& -k_{di}\|r_{ij} + E_{ij}\|^2 \\ \le& k_{di}(-\|r_{ij}\|^2 + \delta\|r_{ij}\|^2 + \frac{1}{\delta}\|E_{ij}\|^2 - \|E_{ij}\|^2),\end{aligned} \tag{61}$$

$$\|K_{pj}R_{ij}^T E_{ij}\| \le \frac{\delta}{2}\|R_{ij}\|^2 + \frac{K_{pj}^2}{2\delta}\|E_{ij}\|^2, \tag{62}$$

By using (61)–(62), similar to the case of $j = 1$, the time derivative of W_j for $j = 2, \ldots, p_i$ can be upper bounded as:

$$\dot{W}_j \le -\frac{\bar{\phi}_j}{\lambda_2}W_j + \varsigma_j, \tag{63}$$

provided that conditions (34)–(37) are satisfied, where

$$\phi_j = \min_{i=m,\ s}\left\{l_{ij}(\alpha - \frac{\delta}{2}l_{ij}),\ k_a - \frac{\delta}{2},\ \frac{\kappa}{\bar{\zeta}_i K_{pj}^2} - \frac{3}{2\delta} - \gamma_1^2 - \gamma_2^2\right\}, \tag{64}$$

$$\bar{\phi}_j = \min_{i=m,\ s}\left\{\phi_j - \frac{\rho_j^2(\|z_j\|)}{2k_b},\ \frac{\gamma_1^2}{\kappa},\ \frac{\bar{\zeta}_i\gamma_2^2}{\omega}\right\}. \tag{65}$$

$$\varsigma_j = \frac{v^2}{2k_c} + (\frac{k_{pj}^2}{2\delta} + \frac{1}{\delta} - 1)(\|E_{mj}\|^2 + \|E_{sj}\|^2). \tag{66}$$

If $R_{i,j-1}$, $e_{i,j-1}$, and $\theta_{i,j-1}$ are bounded, then according to the definitions in (29) and (33), $\eta_{i,j-1}$ and E_{ij} are also bounded variables. By utilizing the comparison lemma, we can obtain W_j will converge into the bounded regions. Then through combining the results with the first step, the prediction errors R_{ij}, e_{ij}, and η_{ij} converge to the bounded regions for $j = 1, 2, \ldots, p_i$.

The proof of Theorem 1 is ended.

From Eq. (66), the prediction errors which is caused by v could be made sufficiently small by applying high values of the predictor gain K_{pi}. By this way, however, the upper bounds of prediction horizons ζ_{ij} should be small enough according to (37). According to the definitions of ζ_{ij} in (14), the upper bound of ζ_{ij} is related to the numbers of sub-observers p_i. As long as p_i is sufficient large, $\bar{\zeta}_{ij}$ can be small enough. In other words, we should use more sub-predictors to apply a higher value of the

predictor gain and achieve smaller prediction errors, which will lead to increasing calculation costs of the predictors at the same time.

In general case, in order to find a suitable (not too redundant) p_i, we might have to calculate ζ_{ij} multiple times in (14) with different p_i, and then obtain the upper bound $\bar{\zeta}_{ij}$ to verify the condition (37). However, if the delay is slowly varying or the number of sub-predictors is very large, then there is $\zeta_{ij}(t) \approx \frac{1}{p_i}\tau(t)$. To reduce complex calculations, we can approximately apply $\zeta_{ij} = \frac{\tau_0}{p_i}$ into the conditions (37) to preliminarily determine the p_i. If this initial value of p_i is invalid, then we should use more sub-observers.

Remark 4. Because the domain of the integral is time-varying, the main difficulty of implementation of the proposed predictor is the computation of $\theta_{ij}(t-\zeta_{ij}(t))$. After differentiating with respect to time, we have $(1-\dot{\zeta}_{ij})\dot{\theta}_{ij}(t-\zeta_{ij}) = (1-\dot{\zeta}_{ij})[r_{ij\zeta} - (1-\dot{\zeta}_{ij}(t-\zeta_{ij}))r_{ij\zeta}(t-\zeta_{ij})]$. Thus, optionally, we can take the time integral of the right hand to calculate $\theta_{ij}(t-\zeta_{ij}(t))$.

Remark 5. If the velocities of robot system are not measured, we can use a velocity observer [7,19] ahead of the cascade predictor (as the zeroth sub-predictor) to obtain estimated value of $\dot{q}_i(t-\tau_i)$. As long as that estimation errors of the velocity observer are bounded, according to the previous analysis, the prediction errors are still bounded.

Proposition 1 (*Uncertainty-free Case*). *If the dynamic models of the human force and environment force $f_i(q_i,\ \dot{q}_i)$ are known, and there is no uncertainty and disturbance ($\varepsilon_i = 0$) in the system (1), the cascade predictor (20)–(21) turns into*

$$\dot{x}_{1ij}(t) = l_{ij}(t)x_{2ij}(t), \tag{67}$$

$$\begin{aligned}\dot{x}_{2ij}(t) =& l_{ij}(t)[g_i(x_{1ij}(t), x_{2ij}(t)) + \hat{M}_i^{-1}(x_{1ij}(t))\hat{u}_{ij}(t) + f_i(x_{1ij}, x_{2ij})] \\ &+ K_{pi}(1-\dot{\zeta}_{ij}(t))r_{ij\zeta}(t),\end{aligned} \tag{68}$$

And if the conditions in (34)–(37) are satisfied, then the prediction errors R_{ij}, e_{ij}, and η_{ij} converge to be zero exponentially. The proof is shown in the Appendix.

4. Bilateral controller design based on prediction results

By applying the prediction results, the following bilateral predictive controller is designed:

$$u_m = -K_f\hat{u}_s - B_m\dot{q}_m, \tag{69}$$

$$u_s = K_s(x_{1mp} - q_s) - B_s\dot{q}_s. \tag{70}$$

where K_f, K_s, B_m, B_s are controller gains, and $\hat{u}_s$ represents the predicted torque feedback, which is calculated as

$$\hat{u}_s = K_s(q_m - x_{1sp}) - B_s x_{2sp}. \tag{71}$$

In order to achieve approximate real-time motion synchronization and feedback, distinguished from the similar controller proposed in [22], the prediction results are applied into our approach to replace the delayed measurements.

Theorem 2. *The controller described by (69)–(70) and the predictor described by (20)–(21) ensure the boundness of $\dot{q}_i$ and $q_m - q_s$ for the teleoperation system (1), provided that the controller gains satisfy the following conditions simultaneously:*

$$B_m > \frac{1}{2\delta}K_f^2(K_s^2 + (\alpha^2+3)B_s^2), \tag{72}$$

$$K_f B_s > \frac{1}{2\delta}K_s^2K_f^2 + \frac{\delta}{2}, \tag{73}$$

$$\alpha > \frac{3\delta}{2},\quad \frac{\delta}{2\omega} < 1-\dot{\zeta},\quad \bar{\zeta}_i < \frac{2\kappa\delta}{(3+\delta^2)K_{pi}^2}, \tag{74}$$

$$k_a > \delta,\quad k_b \geq \frac{\rho_j^2(\|z_p(0)\|)}{2\Phi_p},\quad k_{di} > \frac{\delta + 2\omega + 2\kappa\bar{\zeta}_i}{2(1-\delta)}, \tag{75}$$

where

$$\Phi_j = \min_{i=m,\ s}\left\{\alpha - \frac{3}{2}\delta,\ k_a - \delta,\ \frac{\kappa}{\bar{\zeta}_i K_{pj}^2} - \frac{3}{2\delta} - \frac{\delta}{2} - \gamma_1^2 - \gamma_2^2\right\}. \tag{76}$$

Proof of Theorem 2. Based on Eq. (45), we establish the Lyapunov functional as below:

$$V = V_c(t) + W_{j=p} = V_c + V_{mp} + V_{sp} \tag{77}$$

$$V_c(t) = \frac{1}{2}\dot{q}_m^T M_m(q_m)\dot{q}_m + \frac{1}{2}K_f\dot{q}_s^T M_m(q_s)\dot{q}_s + \frac{K_fK_s}{2}(q_m - q_s)^2. \tag{78}$$

where W_j, V_{mj} and V_{sj} were defined in Eqs. (45) and (46).

The time derivative of V_c can be derived by applying property 3 as

$$\begin{aligned}\dot{V}_c =& \dot{q}_m^T[u_m + \varepsilon_m + f_m + K_fK_s(q_m - q_s)] \\ &+ \dot{q}_s^T[K_f u_s + K_f\varepsilon_s + K_f f_s - K_fK_s(q_m - q_s)] \\ =& -B_m\|\dot{q}_m\|^2 + \dot{q}_m^T(\varepsilon_m + f_m) - K_fK_s\dot{q}_m^T e_{sp} - K_fB_s\dot{q}_m^T x_{2sp} \\ &- K_fB_s\|\dot{q}_s\|^2 + K_f\dot{q}_s^T(\varepsilon_s + f_s) - K_sK_f\dot{q}_s^T e_{mp}.\end{aligned} \tag{79}$$

Using the relationship $x_{2sp} = \dot{q}_s - \eta_{sp} = \dot{q}_s - (R_{sp} - \alpha e_{sp} - \theta_{sp})$ and Young's inequality, we can derive

$$\|K_fK_s\dot{q}_m^T e_{sp}\| \leq \frac{1}{2\delta}(K_fK_s)^2\|\dot{q}_m\|^2 + \frac{\delta}{2}\|e_{sp}\|^2, \tag{80}$$

$$\begin{aligned}\|K_fB_s\dot{q}_m^T x_{2sp}\| \leq& \frac{(3+\alpha^2)K_f^2B_s^2}{2\delta}\|\dot{q}_m\|^2 \\ &+ \frac{\delta}{2}\|\dot{q}_s\|^2 + \frac{\delta}{2}\|R_{sp}\|^2 + \frac{\delta}{2}\|e_{sp}\|^2 + \frac{\delta}{2}\|\theta_{sp}\|^2,\end{aligned} \tag{81}$$

$$\|K_sK_f\dot{q}_s^T e_{mp}\| \leq \frac{1}{2\delta}(K_sK_f)^2\|\dot{q}_s\|^2 + \frac{\delta}{2}\|e_{mp}\|^2, \tag{82}$$

Substituting (80)–(82) into (79), we can obtain

$$\begin{aligned}\dot{V}_c \leq& -(B_{ma} - \frac{1}{2\delta}K_f^2(K_s^2 + (3+\alpha^2)B_s^2))\|\dot{q}_m\|^2 + \frac{v_1^2}{4B_{mb}} \\ &- (K_fB_{sa} - \frac{1}{2\delta}K_s^2K_f^2 - \frac{\delta}{2})\|\dot{q}_s\|^2 + \frac{K_fv_1^2}{4B_{sb}} \\ &+ \frac{\delta}{2}(\|e_{mp}\|^2 + 2\|e_{sp}\|^2 + \|R_{sp}\|^2 + \|\theta_{sp}\|^2),\end{aligned} \tag{83}$$

where $B_m = B_{ma} + B_{mb}$, $B_s = B_{sa} + B_{sb}$. Then substituting (83) and (63) into (77) and completing the squares, and noticing that $l_{i,j=p} = 1$, we have

$$\dot{V} \leq -\frac{\bar{\Phi}_p}{\lambda_3}V + \bar{\eta}. \tag{84}$$

where $\lambda_3 = \max_{i=m,\ s}\left\{1,\ \frac{1}{2K_{pi}},\ \frac{K_fK_s}{2}\right\}$,

$$\bar{\eta} = \frac{v^2}{2k_c} + (\frac{k_{pj}^2}{2\delta} + \frac{1}{\delta} - 1)(\|E_{mj}\|^2 + \|E_{sj}\|^2) + \frac{v_1^2}{4B_{mb}} + \frac{K_fv_1^2}{4B_{sb}} \tag{85}$$

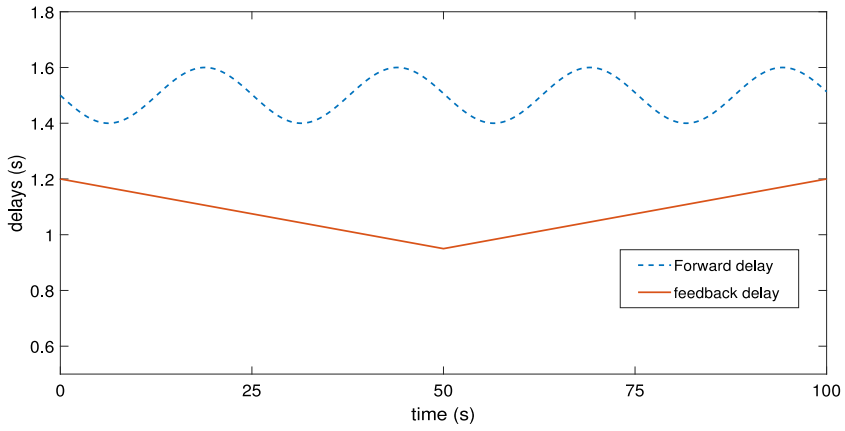

Fig. 4. Time delays.

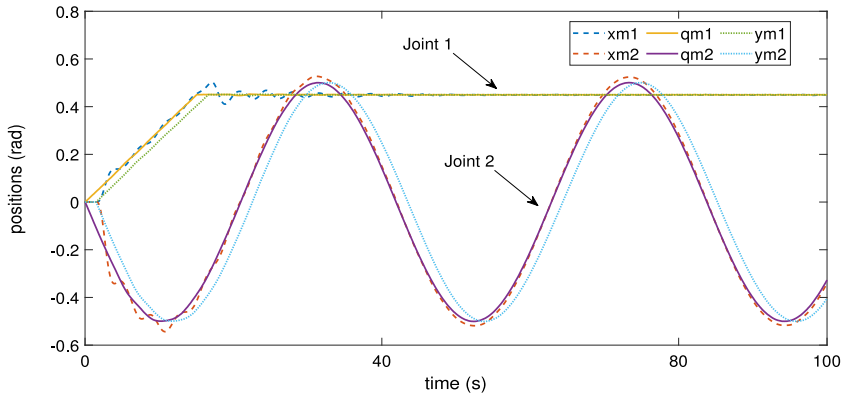

Fig. 5. Predicted results of joint positions of master robot.

Table 1
Parameters and control gains of teleoperation system.

π_1	π_2	α	K_{pm}	K_{ps}	K_s
1 kg	0.5 kg	1	10	5	10 kg/s^2
ι_1	ι_2	K_f	B_m	B_s	
0.5 m	0.5 m	0.1	2 kg/s	1 kg/s	

$$\bar{\Phi}_p = \min_{i=m,\ s}\left\{\Phi_p - \frac{\rho_j^2(\|z_p\|)}{2k_b},\ \frac{\gamma_1^2}{\kappa},\ \frac{\bar{\zeta}_i\gamma_2^2}{\omega},\right.$$
$$\left. B_{ma} - \frac{1}{2\delta}K_f^2(K_s^2+(3+\alpha^2)B_s^2),\ K_fB_{sa} - \frac{1}{2\delta}K_s^2K_f^2 - \frac{\delta}{2}\right\}. \tag{86}$$

Using the comparison lemma, there is

$$V \le V(0)e^{-\frac{\bar{\Phi}_p}{\lambda_3}t} + \frac{\lambda_3}{\phi_2}\bar{\eta}. \tag{87}$$

According to the definition of V, we can conclude $\dot{q}_i$ and $q_m - q_s$ are bounded.

The proof of Theorem 2 is accomplished.

In general, the Lyapunov based stability conditions are very conservative because the worst case scenarios have been considered. Even then, these conditions can provide some important guidance when we design the controller. It can be concluded from conditions (72)–(73) that B_m, B_s should be big enough when the gains K_f and K_s are high. And according to inequalities (74), the choice of α is relatively free via using a appropriate value of δ.

Remark 6. The proposed predictor–controller structure for teleoperation system is differ from common observer-based output-feedback controller design. The predicted positions of one robot (master or slave) are applied to another robot instead of being fed back to itself. Thus the stability results are different from the separation principles such as in [29].

5. Simulations

In this part, several simulations are carried out by using a 2-DOF teleoperation system. The mathematical model of master and slave are same which is given as

$$M_i(q) = \begin{bmatrix}(2\iota_1\cos q_2 + \iota_2)\iota_2\pi_2 + (\pi_1+\pi_2)\iota_1^2 & \iota_2^2\pi_2 + \iota_1\iota_2\pi_2\cos q_2\\ \iota_2^2\pi_2 + \iota_1\iota_2\pi_2\cos q_2 & \iota_2^2\pi_2\end{bmatrix},$$
$$C_i(q,\dot{q}) = \begin{bmatrix}-(\iota_1\iota_2\pi_2\dot{q}_2)\sin q_2 & -[\iota_1\iota_2\pi_2(\dot{q}_1+\dot{q}_2)]\sin q_2\\ (\iota_1\iota_2\pi_2\dot{q}_1)\sin q_2 & 0\end{bmatrix},$$

The master robot is assumed to be handled by the operator to follow given trajectories. Thus the input force of the operator is established as a PD controller under the disturbance, i.e. $f_m = 10(\dot{q}_m-\dot{q}_d)+50(q_m-q_d)+w$, and $w \sim [0,\ 10^{-3}]$ represent a Gaussian noise, $q_d = \begin{bmatrix}q_{d1}^T & q_{d2}^T\end{bmatrix}^T$, and $q_{d1} = \begin{cases}0.03t, & 0 \le t \le 15,\\ 0.45, & t \ge 15\end{cases}$, $q_{d2} = -0.5\sin(0.15t)$. The environment force is modeled as $f_s = 0.01\dot{q}_s + 0.05\sin(q_s)$. And the time delays are simulated as $\tau_m = 1.5+0.1\sin(0.25t)$ second, and $\tau_s = \begin{cases}1.2-0.005t, & 0 \le t \le 50,\\ 0.95+0.005t, & t \ge 50.\end{cases}$

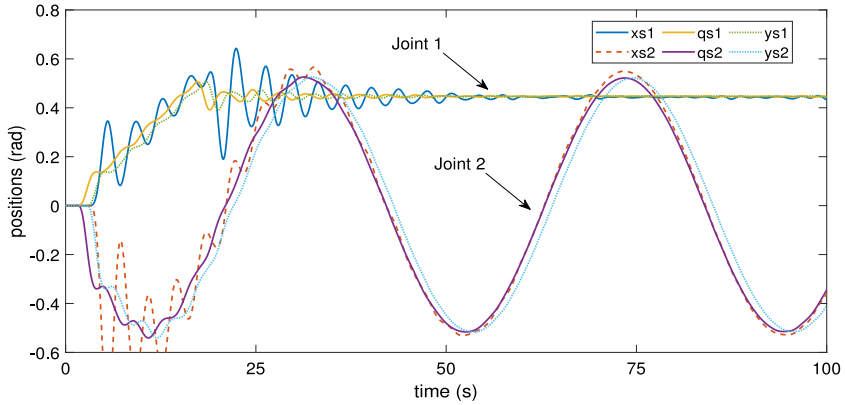

Fig. 6. Predicted results of joint positions of slave robot.

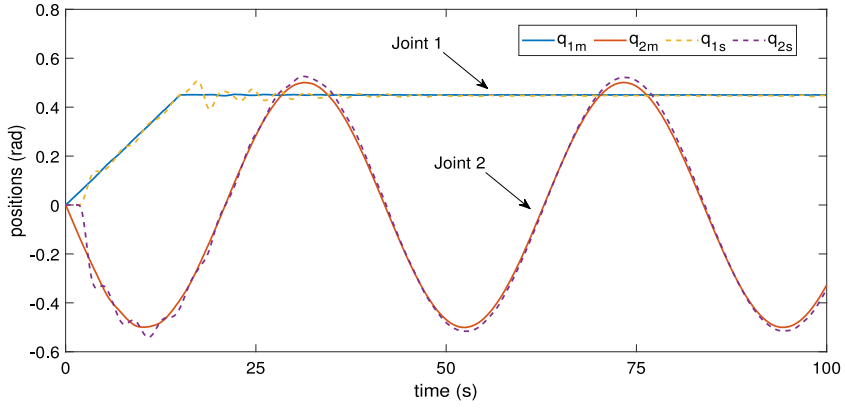

Fig. 7. Position tracking performance of teleoperation system.

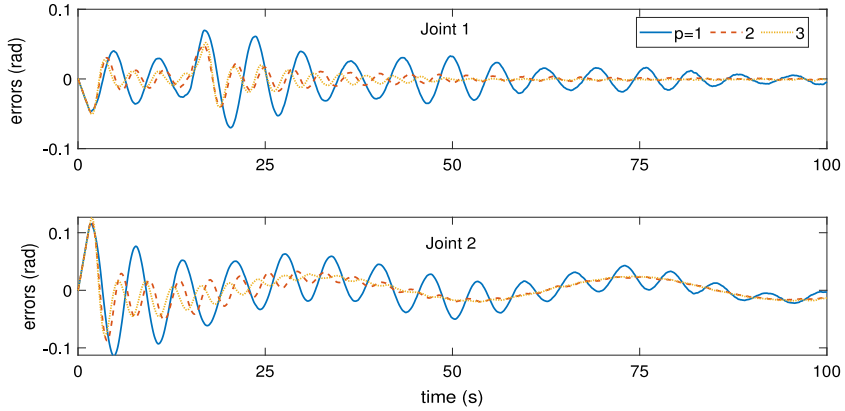

Fig. 8. Prediction errors for master robot with different numbers of predictors.

which is shown in Fig. 4. The parameters of robots and controllers are given in Table 1. To testify the robustness to model uncertainties of proposed approach, the estimated function is selected as $h_i(x_{ij}, \dot{x}_{ij}) + \hat{M}_i^{-1}(x_{ij})\hat{u}_{ij} = 0$ in the predictor.

Scenario 1: Firstly, we apply $p_m = p_s = 3$ sub-predictors in the cascade on both slave and master sides. Figs. 5 and 6 present the prediction results of positions of robots on both two sides. It is obvious that the predicted positions (xm1, xm2, xs1 and xs2) are closer to the real ones (qm1, qm2, qs1, and qs2) than the delayed measurements (ym1, ym2, ys1, ys2). Then, Fig. 7 gives the position synchronization performance of teleoperation system. As illustrated in the presented figures, our method can achieve the good performances under time-varying delays and model uncertainties.

Scenario 2: Next, the numbers of sub-predictors are chosen as $p_m = p_s = 1, 2, 3$, respectively. The comparative results of prediction errors with different p_i on both sides are shown in Figs. 8 and 9, respectively. As it is analyzed earlier, the prediction errors get smaller when more sub-predictors are used.

Scenario 3: Finally, we compare the proposed variable prediction horizon method with the output reconstruction method [20], which turn the system output into constant delay case through further artificially delaying the measurement. The numbers of sub-predictors of both two methods are chosen as $p_m = p_s = 3$.

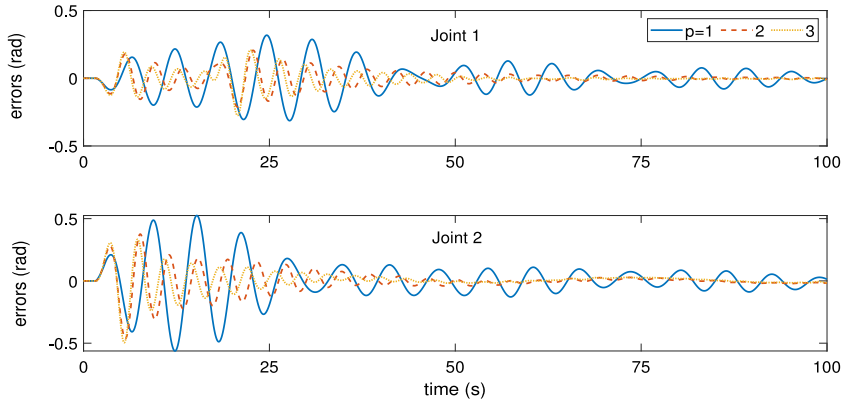

Fig. 9. Prediction errors for slave robot with different numbers of predictors.

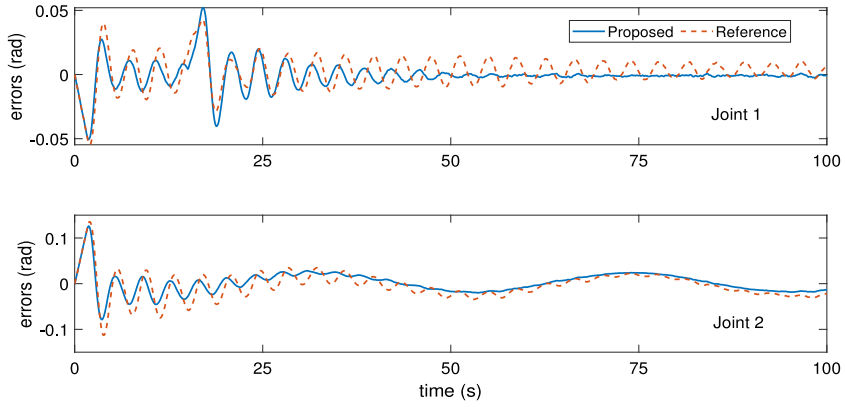

Fig. 10. Comparative prediction errors of master robot with different predictors.

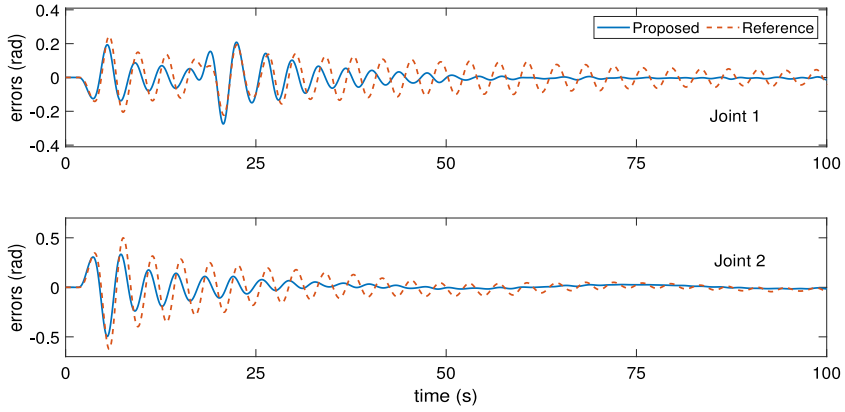

Fig. 11. Comparative prediction errors of slave robot with different predictors.

In Figs. 10 and 11, the comparative results of prediction errors of two methods are presented. Because the communication delays are artificially increased, the prediction errors also rise by using the output reconstruction method. Better performance of proposed method in our paper can be shown.

6. Conclusions

A predictor-based motion control approach for teleoperation system has been developed in this paper. The actual states of robots on both sides have been estimated by novel robust cascade predictors through using the delayed measurements. By applying several chained sub-predictors with variable prediction horizons, the proposed predictor is suitable for the long time-varying delay case. In addition, we employed an estimated input functions instead of the real controller input which was unavailable on the same side of the predictors. This features of our work can greatly improve the easiness of the implementation of proposed predictors for teleoperation system. After utilizing the predictions to design the controller, almost real-time information exchange and motion synchronization can be achieved. The better performance of proposed method has been proved by some simulations by comparing with other methods. Further studies will be focused on the predictor designs with unknown time-delays and compensation methods for uncertainties. In addition, the extensions of proposed prediction method to the constraint control cases [3]

are also important and interesting research topic in our future works.

Declaration of competing interest

The authors declare that they have no known competing financial interests or personal relationships that could have appeared to influence the work reported in this paper.

Acknowledgments

This work was supported by the National Key Research and Development Program of China under Grant No.2016YFB1001301, and the Key Program of the National Natural Science Joint Foundation of China under Grant No.U1713210.

Appendix. Proof of Proposition 1

Proof. In the uncertainty-free case, we have

$$N_{dij} = 0, \tag{A.1}$$

$$N_{ij} = l_{ij}[g(q_{ij}, \dot{q}_{ij}) - g(x_{1ij}, x_{2ij})] + \alpha \dot{e}_{ij} + e_{ij} + l_{ij}[M_i^{-1}(q_{ij})(u_{ij} + f_i(q_{ij}, \dot{q}_{ij})) - M_i^{-1}(x_{1ij})(\hat{u}_{ij} + f_i(x_{1ij}, x_{2ij}))]. \tag{A.2}$$

Then following the proof of Theorem 1, for $j = 1$, it can be derived that

$$\dot{W}_1 \leq -\frac{\bar{\phi}_1}{\lambda_2} W_1 \tag{A.3}$$

Thus R_{i1}, e_{i1}, and θ_{ij} converge to be zero exponentially, provided that all the same conditions (34)–(37) in Theorem 1 are satisfied.

Likewise, for $j = 2, \ldots, p_i$, we have

$$\dot{W}_j \leq -\frac{\bar{\phi}_j}{\lambda_2} W_j + (\frac{k_{pj}^2}{2\delta} + \frac{1}{\delta} - 1)(\|E_{mj}\|^2 + \|E_{sj}\|^2). \tag{A.4}$$

If $R_{i,j-1}$, $e_{i,j-1}$, and $\theta_{i,j-1}$ converge to be zero exponentially, then according to the definitions in (29) and (33), $\eta_{i,j-1}$ and E_{ij} also converge to be zero exponentially. Using the comparison lemma, we can conclude W_j will converge to be zero in an exponential way. By combining with the results of $j = 1$, the proof of Proposition 1 is completed.

References

[1] Luo J, Yang C, Wang N, Wang M. Enhanced teleoperation performance using hybrid control and virtual fixture. Internat J Systems Sci 2019;50(3):451–62.
[2] Amini H, Farzaneh B, Azimifar F, Sarhan A. Sensor-less force-reflecting macro–micro telemanipulation systems by piezoelectric actuators. ISA Trans 2016;64:293–302.
[3] Wang Z, Liang B, Sun Y, Zhang T. Adaptive fault-tolerant prescribed-time control for teleoperation systems with position error constraints. IEEE Trans Ind Inf 2020;16(7):4889–99.
[4] Zakerimanesh A, Hashemzadeh F, Ghiasi AR. Dual-user nonlinear teleoperation subjected to varying time delay and bounded inputs. ISA Trans 2017;68:33–47.
[5] Slawiński E, Santiago D, Mut V. Control for delayed bilateral teleoperation of a quadrotor. ISA Trans 2017;71:415–25.
[6] Niemeyer G, Slotine J-J. Stable adaptive teleoperation. IEEE J Ocean Eng 1991;16(1):152–62.
[7] Hua C, Liu XP. Teleoperation over the internet with/without velocity signal. IEEE Trans Instrum Meas 2010;60(1):4–13.
[8] Zhai D-H, Xia Y. Adaptive finite-time control for nonlinear teleoperation systems with asymmetric time-varying delays. Internat J Robust Nonlinear Control 2016;26(12):2586–607.
[9] Wang Z, Sun Y, Liang B. Synchronization control for bilateral teleoperation system with position error constraints: A fixed-time approach. ISA Trans 2019;93:125–36.
[10] Uddin R, Ryu J. Predictive control approaches for bilateral teleoperation. Annu Rev Control 2016;42:82–99.
[11] Rubagotti M, Taunyazov T, Omarali B, Shintemirov A. Semi-autonomous robot teleoperation with obstacle avoidance via model predictive control. IEEE Robot Autom Lett 2019;4(3):2746–53.
[12] da Cunha Pereira Pinto HL, Oliveira TR, Hsu L. Sliding mode observer for fault reconstruction of time-delay and sampled-output systems–a time shift approach. Automatica 2019;106:390–400.
[13] Kamalapurkar R, Fischer N, Obuz S, Dixon WE. Time-varying input and state delay compensation for uncertain nonlinear systems. IEEE Trans Automat Control 2015;61(3):834–9.
[14] Obuz S, Klotz JR, Kamalapurkar R, Dixon W. Unknown time-varying input delay compensation for uncertain nonlinear systems. Automatica 2017;76:222–9.
[15] Zhang J, Lin Y, Shi P. Output tracking control of networked control systems via delay compensation controllers. Automatica 2015;57:85–92.
[16] Shen S, Song A, Li T. Predictor-based motion tracking control for cloud robotic systems with delayed measurements. Electronics 2019;8(4):398.
[17] Ahmed-Ali T, Cherrier E, Lamnabhi-Lagarrigue F. Cascade high gain predictors for a class of nonlinear systems. IEEE Trans Automat Control 2011;57(1):221–6.
[18] Germani A, Manes C, Pepe P. A new approach to state observation of nonlinear systems with delayed output. IEEE Trans Automat Control 2002;47(1):96–101.
[19] Farza M, Hernández-González O, Menard T, Targui B, M'saad M, Astorga-Zaragoza C-M. Cascade observer design for a class of uncertain nonlinear systems with delayed outputs. Automatica 2018;89:125–34.
[20] Farza M, M'Saad M, Menard T, Fall ML, Gehan O, Pigeon E. Simple cascade observer for a class of nonlinear systems with long output delays. IEEE Trans Automat Control 2015;60(12):3338–43.
[21] Tréangle C, Farza M, M'Saad M. Observer design for a class of disturbed nonlinear systems with time-varying delayed outputs using mixed time-continuous and sampled measurements. Automatica 2019;107:231–40.
[22] Nuño E, Ortega R, Barabanov N, Basañez L. A globally stable PD controller for bilateral teleoperators. IEEE Trans Robot 2008;24(3):753–8.
[23] Hua C-C, Liu XP. Delay-dependent stability criteria of teleoperation systems with asymmetric time-varying delays. IEEE Trans Robot 2010;26(5):925–32.
[24] Hashemzadeh F, Hassanzadeh I, Tavakoli M. Teleoperation in the presence of varying time delays and sandwich linearity in actuators. Automatica 2013;49(9):2813–21.
[25] Zhang H, Song A, Shen S. Adaptive finite-time synchronization control for teleoperation system with varying time delays. IEEE Access 2018;6:40940–9.
[26] Yang H, Liu L, Wang Y. Observer-based sliding mode control for bilateral teleoperation with time-varying delays. Control Eng Pract 2019;91:104097.
[27] Kebria PM, Khosravi A, Nahavandi S, Shi P, Alizadehsani R. Robust adaptive control scheme for teleoperation systems with delay and uncertainties. IEEE Trans Cybern 2019;1–11.
[28] Khalil HK. Nonlinear systems. Upper Saddle River; 2002.
[29] Khalil HK. Cascade high-gain observers in output feedback control. Automatica 2017;80:110–8.